Electrical Engineering in Japan, Vol. 161, No. 3, 2007
Translated from Denki Gakkai Ronbunshi, Vol. 126-C, No. 5, May 2006, pp. 579–588

A Kinematic and Dynamic Analysis on Orthotic Gait of Paraplegics

TAKAHIRO KAGAWA,[1,*] HIROSHI FUKUDA,[2] and YOJI UNO[3]
[1]Keio University, Japan
[2]Toyohashi University of Technology, Japan
[3]Nagoya University, Japan

SUMMARY

In this study, we attempt to quantify the relationship between significant arm-clutch loading, leg restriction, and motor paralysis, and analyze lumbar joint trajectories in the orthotic gait of paraplegic subjects and in the ordinary and orthotic gaits of a normal subject, by using an inverted pendulum model. With leg restriction, the trajectories are located in front of an equilibrium point of the inverted pendulum, and the loading is higher due to the influence of the gravity moment. Comparing the trajectories of paraplegic and normal gait with orthosis in the horizontal plane, the trajectory in the paraplegic subjects was rectilinear, while that in the normal subject was curved in the direction toward the equilibrium point. The loading is lower in the curved trajectory than in the straight trajectory because of the trade-off between gravity and inertia. These results suggest that the increase in the distance between the trunk movement and the equilibrium point of the inverted pendulum results in significant loading due to leg restriction and motor paralysis in the orthotic gait of paraplegics. © 2007 Wiley Periodicals, Inc. Electr Eng Jpn, 161(3): 10–21, 2007; Published online in Wiley InterScience (www.interscience.wiley.com). DOI 10.1002/eej.20533

Key words: paraplegics; orthosis; gait analysis; inverted pendulum model.

1. Introduction

Patients with spinal cord injury (SCI) cannot activate the muscles related to the injured spinal block. Injury of a high spinal block results in a large region of paralysis, affecting not only the leg muscles but also the trunk muscles. Although most SCI patients use a wheelchair for mobility, life in a wheelchair often results in a reduction of musculoskeletal functions, such as joint contracture, muscle atrophy, spasticity, osteoporosis, and subsequent fractures of the lower extremities. To maintain and improve musculoskeletal functions, loading the paralyzed lower extremities and expanding the range of motion are important considerations [1–3].

To prevent secondary complications, paraplegics are trained to walk and stand wearing an orthosis that enables standing and ambulation for short distances by restricting the movements of the paralyzed joints. Hip-knee-ankle-foot orthoses (HKAFO), such as the reciprocating gait orthosis (RGO) or ParaWalkers, are among the most common types of orthoses [4, 5]. In HKAFO, a pelvic band supports the trunk; these have been used for high thoracic SCI. However, it is difficult for patients to put on an orthosis by themselves and they require a significant amount of assistance. On the other hand, knee-ankle-foot orthoses with a medial-single-hip joint (MSH-KAFO) are orthoses without pelvic bands; these have the advantage that paraplegic patients can put them on by themselves while seated in a wheelchair [3, 6]. MSH-KAFOs have been used with lower thoracic SCI because the paralyzed thoracic, lumbar, and hip joints are not restricted. To support their independent lives, reduced assistance is desirable. Therefore, we address an orthotic gait using the MSH-KAFO.

Although a paraplegic can walk with an orthosis and a pair of crutches, the distance of continuous ambulation is short due to high arm loading. The hand pain due to the high reaction force of crutches is also one of the factors limiting the walking distance. Nene and Major evaluated the ground

---

[*] Current address: Tsukigase Rehabilitation Center

Contract grant sponsor: “Basic Technology Development for Practical Application of Human Support Robots” program of the New Energy and Industrial Technology Development Organization (NEDO) and the 21st Century COE Program “Intelligent Human Sensing” of the Ministry of Education, Culture, Sports, Science and Technology of Japan.

© 2007 Wiley Periodicals, Inc.

reaction force patterns during paraplegic gait with HKAFO [7]. They showed that crutch loading increased during the single support phase, and concluded that the bending of a pelvic band by the lateral trunk movement would induce a large burden for paraplegics. Jefferson and Whittle compared three types of HKAFO with respect to gait kinematics. In all types, the lateral movement of the pelvis is significantly greater than in the normal gait [8]. The lateral movement of the pelvis is caused by interference with foot-floor clearance due to the fixation of the knee joint at the complete extension position. Although the orthotic gait of paraplegics has been evaluated kinematically or dynamically, few studies have assessed both the kinematic and dynamic aspects, which is necessary in order to investigate the efficiency of the gait and to improve the gait pattern and the design of orthotic devices.

In the orthotic gait of paraplegics, significant arm loading is caused by leg restriction and motor paralysis. In the design of a novel gait orthosis or a power assist mechanism, a specification of the joint degrees of freedom would severely affect the gait pattern and the effort of the upper extremities. Therefore, for the improvement of locomotor function by assist devices, it is necessary to assess the influences of the leg restriction and of motor paralysis during the orthotic gait.

In the present study, we analyze the kinematic differences and the influences of gait dynamics induced by leg restriction and motor paralysis. The orthotic gait of paraplegics and normal subjects and ordinary gait of normal subjects were measured to separate the influences of leg restriction and motor paralysis. Comparing the orthotic gaits of paraplegics, we evaluate the influences of leg restriction and motor paralysis. An analysis based on a dynamic model enables us to assess their efficiency in terms of dynamic quantities, and to provide some indicators to improve gait orthoses or power-assist devices. Furthermore, a parametrization of the features of gait kinematics and a model simulation based on the parameters allows a systematic analysis with respect to the influences to be made. However, it is difficult to simulate musculoskeletal dynamics accurately, due to the complexity of the physical constraints and the uncertainty of the physical parameter values, such as the inertial moments of the body segments and the viscoelasticity of the joints in paraplegics. On the other hand, simplified modeling avoids these problems and provides useful suggestions to understand the complex movements [9]. An inverted pendulum model is one of the simplest models to analyze the bipedal gait of humans [10, 11]. During the single support phase, the point of mass of the inverted pendulum is assumed to be the body's center of mass and the pivot point is assumed to be an ankle joint of the supporting leg. Some studies have suggested that the movement of the body's center of mass shows a ballistic trajectory utilizing gravity, and that the external work is small in the ordinary gait of normal humans. In the orthotic gait of paraplegics, the reaction force of crutches can be regarded as external force acting on the point of mass of the inverted pendulum. Therefore, analysis of an inverted pendulum model is effective in quantifying the contribution of the external forces induced by leg restriction and motor paralysis. The lumbar joint position is located near the center of mass position and the movement of the lumbar joint position might strongly affect the arm loading [10]. In this study, we analyze the lumbar joint trajectory using an inverted pendulum model, and assess the influences of leg restriction and motor paralysis on the basis of gait kinematics and dynamics.

2. Experimental Measurement of Gait Movement

2.1 Method

2.1.1 Subjects

Two paraplegic subjects (subjects 1 and 2) and one normal subject (subject 3) participated in this experiment. The levels of injury in subjects 1 and 2 were the 10th thoracic vertebra (T10) and the 6th thoracic vertebra (T6), respectively. Subject 1, a 42-year-old male who was 180 cm tall and weighed 76.1 kg, was 16 years postinjury. Subject 2, a 37-year-old male who was 172 cm tall and weighed 73.1 kg, was 3 years postinjury. Subject 3 had no musculoskeletal or neurological dysfunction. The subjects were informed of the objectives and procedures of the experiments and gave written consent for their participation.

2.1.2 Procedure

The paraplegic subjects walked with a Primewalk-type orthosis and Lofstrand forearm crutches. The ankle joints were restricted in a slightly dorsiflexed position and the knee joints were restricted in the completely extended position with the orthosis. The hip joints were not restricted to extension/flexion movement. As shown in Fig. 1, the subjects wore a soft corset in the pelvic position and the movement of the lower joints of the trunk was slightly restricted. The subjects underwent some stretch exercises for contracture of the leg joints and performed some orthotic gait trials before the measurement trials. As shown in the right part of Fig. 1, 15 markers were attached to the subject's body. The marker positions were measured with an OPTOTRAK three-dimensional position measurement device (Northern Digital Inc.) at 100 Hz.

For normal subject 3, gait movements with the following four conditions were measured.

(1) Ordinary gait with stride length of subject 1
(2) Orthotic gait with stride length of subject 1

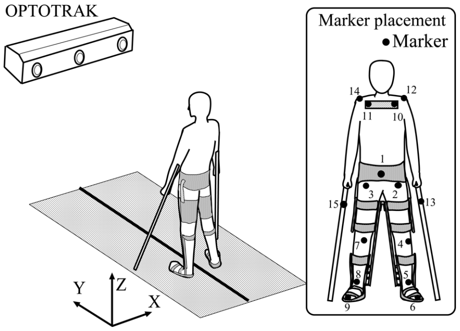
OPTOTRAK
Marker placement
●Marker
14
12
11
10
1
3
2
15
13
7
4
8
5
9
6
Y
Z
X

Fig. 1. Experimental environment.

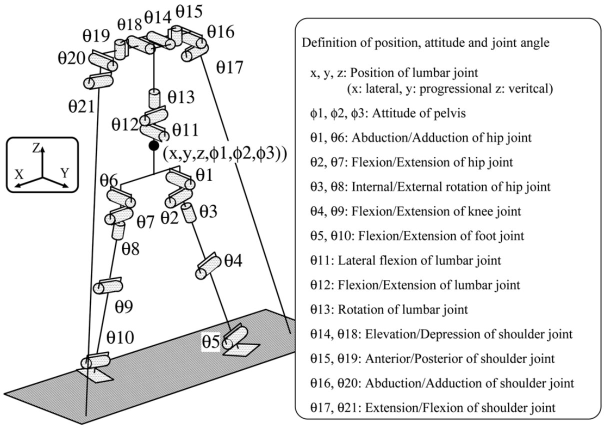
θ19
θ18
θ14
θ15
θ16
θ20
θ17
θ21
θ13
θ12
θ11
(x,y,z,ϕ1,ϕ2,ϕ3))
Z
X
Y
θ6
θ1
θ7
θ2
θ3
θ8
θ4
θ9
θ10
θ5
Definition of position, attitude and joint angle
x, y, z: Position of lumbar joint
(x: lateral, y: progressional z: veritcal)
ϕ1, ϕ2, ϕ3: Attitude of pelvis
θ1, θ6: Abduction/Adduction of hip joint
θ2, θ7: Flexion/Extension of hip joint
θ3, θ8: Internal/External rotation of hip joint
θ4, θ9: Flexion/Extension of knee joint
θ5, θ10: Flexion/Extension of foot joint
θ11: Lateral flexion of lumbar joint
θ12: Flexion/Extension of lumbar joint
θ13: Rotation of lumbar joint
θ14, θ18: Elevation/Depression of shoulder joint
θ15, θ19: Anterior/Posterior of shoulder joint
θ16, θ20: Abduction/Adduction of shoulder joint
θ17, θ21: Extension/Flexion of shoulder joint

Fig. 2. The position, attitude, and joint angle of human skeletal system with crutches.

(3) Ordinary gait with stride length of subject 2
(4) Orthotic gait with stride length of subject 2

Marks indicating the stride length were attached on the walking path. In conditions 1 and 2, the subject wore the Primewalk orthosis but did not wear the corset. As in the case of the paraplegic subjects, the 15 markers were attached to his body and the positions were measured. Since the duration of the double support phase was too short to detect the gait events of heel-contact and toe-off from the measured position data in the ordinary gait, pressure sensors were attached to the shoe soles and the pressure data were measured at 100 Hz.

2.1.3 Analysis

Missing measured position data due to marker occlusion were supplied by using cubic spline interpolation. The measured position data in the orthotic gait of the paraplegic and normal subjects were filtered through a low-pass filter with a cutoff frequency of 5 Hz. The gait events were determined from the velocity of the toe position. In the ordinary gait of the normal subject, the position data were filtered with a cutoff frequency of 10 Hz, since the gait cycle was short. The gait events were detected from the foot pressure data. One-cycle position data from the toe-off to the next toe-off of left foot were segmented. The 15 data sets of one-cycle time series were chosen at random.

The duration of the gait cycle, the stride length, and the gait velocity were calculated from the 15 data sets. For examination of the control of the stride length, a one-way analysis of variance (ANOVA) was performed. The level of significance was set at $p < 0.05$.

As shown in Fig. 2, a geometric human body model with 12 rigid body segments and 21 joints was defined to assess the joint angles of each condition and to reconstruct the movement of the joint positions and body segments. The joint positions and joint angles were calculated on the basis of a homogeneous transform representation (see Appendix 1) [12]. We addressed the movement of the lumbar joint represented as (x, y, z) in Fig. 2. This position corresponded to the lower block of the lumbar spine (from T3 to T5). The 15 trajectories of the lumber joint were normalized to the mean gait cycle by cubic spline interpolation. Subsequently, the normalized trajectories were averaged and the mean trajectory was calculated by a fifth-order Fourier series approximation to satisfy boundary equivalence.

2.2 Results

2.2.1 Spatial and temporal parameters

The mean and SD values of the gait cycle, the durations of the gait phases, the stride length, and the velocity are shown in Table 1. The results of ANOVA indicated no significant difference of stride length between the orthotic gait of paraplegic subject 1 and conditions 1 and 2 of the normal subject [left leg: $F(2, 42) = 2.61$, $P = 0.085$, right leg: $F(2, 42) = 1.03$, $P = 0.36$]. In addition, no significant difference was found between paraplegic subject 2 and conditions 3 and 4 [left leg: $F(2, 42) = 0.76$, $P = 0.47$, right leg: $F(2, 42) = 2.35$, $P = 0.10$]. The gait cycle of the orthotic gaits of paraplegic and normal subjects is larger and the velocity is lower than that of the ordinary gait of the normal subject. Comparing the duration of the gait phase, it was found that the decrease in velocity resulted from an increase in the duration of the double support phase.

2.2.2 Gait kinematics

Stick figures are shown in Fig. 3, where the time interval of the stick diagram is set at 100 ms. The stick figures represent the movements of the body segments during two gait cycles. In the orthotic gait of paraplegic subject 1, the trunk inclined backward during the single support phase and forward during the double support phase. In paraplegic subject 2, the trunk inclination alternated between upright and forward. In the orthotic gait of the

Table 1. Temporal and distance factors in each experimental condition. Numbers in parentheses of first column denote the experimental condition of the normal subject. Values in parentheses of other columns denote standard deviation

	Gait cycle [s]	Duration of gait phases [s]				Stride [cm]		Velocity [m/s]
		Right support	Double support	Left support	Double support	Left	Right	
Subject 1	3.62 (0.13)	1.01 (0.08)	0.87 (0.11)	0.81 (0.02)	0.93 (0.05)	73.6 (9.0)	75.9 (5.6)	0.20 (0.02)
Subject 3(1)	1.32 (0.04)	0.49 (0.02)	0.18 (0.02)	0.48 (0.02)	0.17 (0.02)	76.5 (4.5)	77.9 (4.5)	0.58 (0.03)
Subject 3(2)	2.80 (0.19)	0.78 (0.04)	0.57 (0.11)	0.79 (0.08)	0.60 (0.13)	77.4 (5.0)	76.3 (6.6)	0.27 (0.03)
Subject 2	2.29 (0.15)	0.61 (0.03)	0.53 (0.08)	0.58 (0.04)	0.55 (0.11)	49.9 (7.0)	48.8 (5.0)	0.21 (0.03)
Subject 3(3)	1.25 (0.06)	0.49 (0.04)	0.11 (0.03)	0.54 (0.04)	0.13 (0.02)	45.8 (1.5)	45.8 (2.1)	0.37 (0.02)
Subject 3(4)	2.72 (0.17)	0.62 (0.03)	0.78 (0.11)	0.61 (0.04)	0.76 (0.07)	46.1 (3.8)	45.4 (3.5)	0.16 (0.01)

normal subject, the trunk was kept in a forward inclination. In the ordinary gait of the normal subject (3), the trunk was kept in an upright posture.

The mean lumbar trajectories of each condition are shown in Fig. 4. The figures in the left column show the trajectories in the frontal plane and the right column figures show those in the horizontal plane. Figure 4 shows the trajectories only under large stride conditions because those under small stride conditions are the same as those under large stride conditions. For all conditions, peaks of the vertical displacement were found in the single support phases, and differences in the lateral peaks were found during the double support phases in the orthotic gait of paraplegic subject 1, at toe-off in the orthotic gait of the normal subject (3), and during the single support phases in the ordinary gait of the normal subject. The vertical and lateral displacements were the smallest in the ordinary gait of the normal subject and the largest in the orthotic gait of paraplegic subject 1. The lumbar joint position moved toward the stance leg side at heel contact, and toward the swing leg side in the orthotic gait of paraplegic subject 1. In addition, the shape of the trajectory during the single support phase was rectilinear in the paraplegic subjects, while the trajectories were curved in the orthotic and ordinary gaits of the normal subject with respect to the horizontal plane.

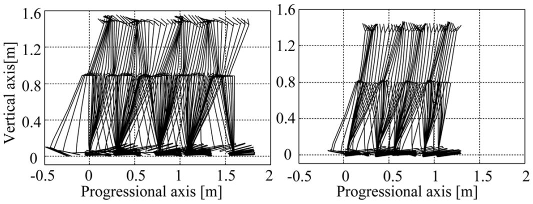

Subject 1 Subject 2

Orthotic gait of paraplegic subjects 1 and 2

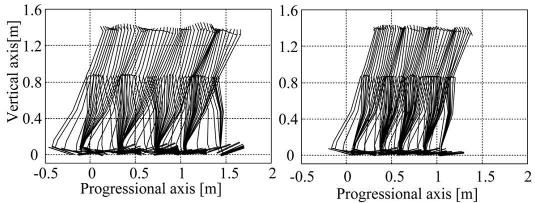

Large stride Small stride

Orthotic gait of normal subject 3

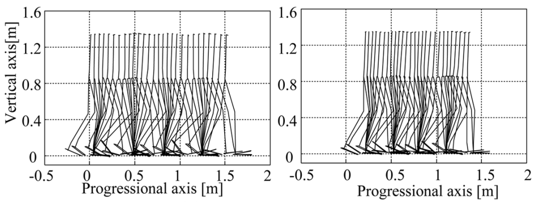

Large stride Small stride

Ordinary gait of normal subject 3

Fig. 3. Stick pictures of the gait in different conditions.

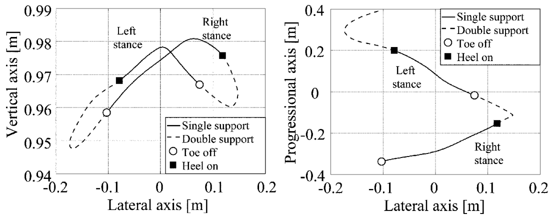

Orthotic gait in paraplegic subject 1

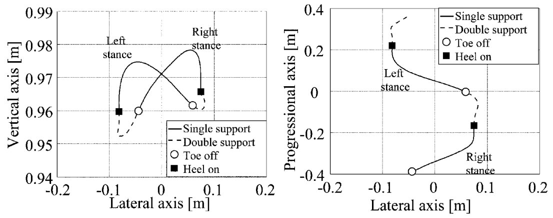

Orthotic gait in normal subject 3

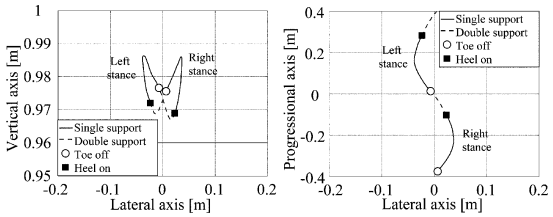

Ordinary gait in normal subject 3

Fig. 4. Lumbar joint trajectories in the frontal plane (left column) and in the horizontal plane (right column).

2.3 Discussion

The velocity of the orthotic gait was lower than that of the ordinary gait of the normal subject. This result suggests that the leg restriction increases the duration of the double support phases and decreases the velocity. The increase of the double support phases might be caused by weight bearing which involves a forward inclination movement of the trunk. This trunk movement would be required to compensate paralyzed leg motor functions such as push-off of the ankle plantar flexor.

The lumbar joint trajectory showed a rectilinear shape in the orthotic gait of the paraplegic subjects, while the trajectories were curved in the ordinary and orthotic gaits of the normal subject during the single support phases. There was a large lateral movement in the orthotic gait performed with the reaction force from crutches. In Section 3, the kinematic differences are analyzed using an inverted pendulum model.

3. Analysis Using an Inverted Pendulum Model

3.1 Method

3.1.1 Analysis of lumbar joint trajectories

As shown in Fig. 5(a), the lumbar joint trajectories during the single support phases were mapped onto the state space of an inverted pendulum model. First, the trajectories were shifted so that the origin corresponded to the ankle joint position. However, a large error between the trajectories and the sphere plane of an inverted pendulum remained. The pivot position of the anterior/posterior direction y_0 was estimated using the least mean squared error because the error would cause progressional displacement of the plantar center of pressure. The equation of the sphere was given as follows:

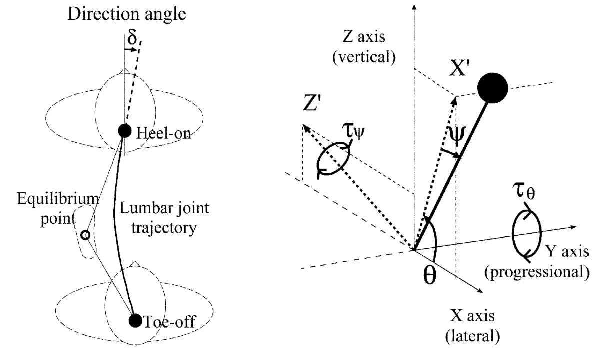

(a) Lumbar joint movement and an inverted pendulum model

(b) Definition of an inverted pendulum model

Fig. 5. An inverted pendulum model.

$$x(i)^2 + \{y(i) - y_0\}^2 + z(i)^2 = L^2 \tag{1}$$

where $x(i)$, $y(i)$, and $z(i)$ denote the lumbar joint positions of the progressional, lateral, and vertical directions, and i denotes the number of time series data. L denotes the radius of the sphere, that is, the distance from the ankle joint to the lumbar joint. Applying least mean squared error estimation, the pivot position y_0 was calculated by the following equation:

$$y_0 = \frac{\sum_{i=1}^{N} \dot{y}(i)\{x(i)\dot{x}(i) + y(i)\dot{y}(i) + z(i)\dot{z}(i)\}}{\sum_{i=1}^{N} \dot{y}^2(i)} \tag{2}$$

In this estimation, the 15 lumbar joint trajectories were used. The mean trajectories were calculated from the 15 trajectories with the origin corresponding to the estimated pivot position.

The definition of an inverted pendulum model is shown in Fig. 5(b). The state variables $\boldsymbol{q} = [\theta, \psi]^T$ are two rotational angles, which are related to Y' and Z' axis as θ. The equation of motion of the inverted pendulum model is

$$\boldsymbol{\tau} = \boldsymbol{M}(\boldsymbol{q})\ddot{\boldsymbol{q}} + \boldsymbol{V}(\boldsymbol{q}, \dot{\boldsymbol{q}}) + \boldsymbol{G}(\boldsymbol{q}) \tag{3}$$

where $\boldsymbol{\tau} = [\tau_\theta, \tau_\psi]^T$ is the torque acting on the joints. We define the joint torques τ_θ and τ_ψ as the lateral torque and progressional torque, respectively. $\boldsymbol{M}$, $\boldsymbol{V}$, and $\boldsymbol{G}$ are the inertial matrix, the Coriolis-centrifugal term, and the gravity term, respectively. The parameter value of the body mass was set as 60 kg and the distance from the ankle joint to the lumbar joint was set as 1.0 m. The position, velocity, and acceleration of θ and ψ were calculated from the mean trajectories, and the torque was calculated from Eq. (3). As the joint torque indicates the magnitude of the external force acting on the mass point of an inverted pendulum, the following cost function is considered as a criterion of the external force contribution:

$$C = \int_0^{T_f} (|\tau_\theta| + |\tau_\psi|) dt \tag{4}$$

where T_f is the movement duration of the single support phase. The cost function has a low value when the trajectory is ballistic and utilizes gravity. The value is increased by utilizing the reaction force of the crutches or other external force.

3.1.2 Analysis of the shape of the lumbar joint trajectories

It was found in the kinematic analysis that the trajectories of the paraplegics had a rectilinear shape and those of the orthotic gait of the normal subject had a curved shape. To compare the external force contribution to the difference of the shape, it is necessary to remove the other differences, such as the position at toe-off or the movement duration, etc. In the lumbar joint trajectories in the horizontal plane, the direction of the trajectories at heel contact reflected the shape of the trajectories. Therefore, we consider the trajectory direction angle δ as the parameter of the trajectory shape. δ was defined as the angle of the velocity direction related to the progressional axis; a positive value indicates the support leg direction and a negative value indicates the opposite of the support leg direction with respect to the lateral displacement.

To calculate a smooth trajectory, which is a feature of human movement, from trajectory direction, a minimum jerk model was used [13]. A minimum jerk trajectory is represented as a fifth-order polynomial function minimizing the integral of the squared acceleration changes during movement. The parameter values of the polynomial function were determined by the boundary conditions, where these conditions were given by the position, velocity, and acceleration of toe-off (initial condition) and heel contact (terminal condition) in the mean trajectory. The direction of the velocity at heel contact was varied according to the parameter value of δ.

3.1.3 Solution of mean trajectory

To calculate the velocity of the state variables at heel contact $\dot{\boldsymbol{q}}_f$, a vector $\boldsymbol{u} = [u_\theta, u_\psi]^T$ specifying the direction of the velocity was determined from the trajectory direction δ. The unit direction vector in the horizontal plane was related to the direction vector of the state variables $\boldsymbol{u}$ by the following equation:

$$\begin{bmatrix} -\sin\delta \\ \cos\delta \end{bmatrix} = \begin{bmatrix} \boldsymbol{J}_{11} & \boldsymbol{J}_{12} \\ \boldsymbol{J}_{21} & \boldsymbol{J}_{22} \end{bmatrix} \begin{bmatrix} u_\theta \\ u_\psi \end{bmatrix} \qquad (5)$$

where $\boldsymbol{J}_{ij}$ denotes the factors of the Jacobian matrix shown in Appendix 2. First, solving Eq. (5), the state velocity vector was obtained. Second, the velocity of the state variables $\dot{\boldsymbol{q}}_f$ was calculated from the tangential velocity $|\dot{\boldsymbol{q}}_f|$ and the direction vector $\boldsymbol{u}$ by using $\boldsymbol{v}_u$, obtained by substituting the direction vector $\boldsymbol{u}$ for $\dot{\boldsymbol{q}}$ in Eq. (A.11), and the tangential velocity $\boldsymbol{v}_f$, as follows:

$$\dot{\boldsymbol{q}}_f = \frac{|\boldsymbol{v}_f|}{|\boldsymbol{v}_u|}\boldsymbol{u} \qquad (6)$$

The trajectories were obtained from the shape parameter and used to evaluate the relationship between the shape of the trajectory and the external force contribution.

3.2 Results

3.2.1 Analysis of the mean trajectories

The trajectories during the left single support phases in the horizontal plane are shown in Figs. 6(a) and 6(b), where thin lines and thick lines indicate the 15 trajectories and the mean trajectory, respectively. In addition, solid lines, dashed lines, and dash-dot lines represent the trajectories of the orthotic gait of the paraplegics, the orthotic gait of the normal subject, and the ordinary gait of the normal subject, respectively. The position (0, 0) is the pivot position of the inverted pendulum. This position also corresponds to the unstable equilibrium point of the inverted pendulum dynamics. The initial positions of the ordinary gait of the normal subject, which correspond to the lumbar joint position at toe-off, located behind the equilibrium point, and the positions at the lateral peak approached the equilibrium point. In the orthotic gaits of the paraplegic and normal subjects, the initial positions are located more to the front

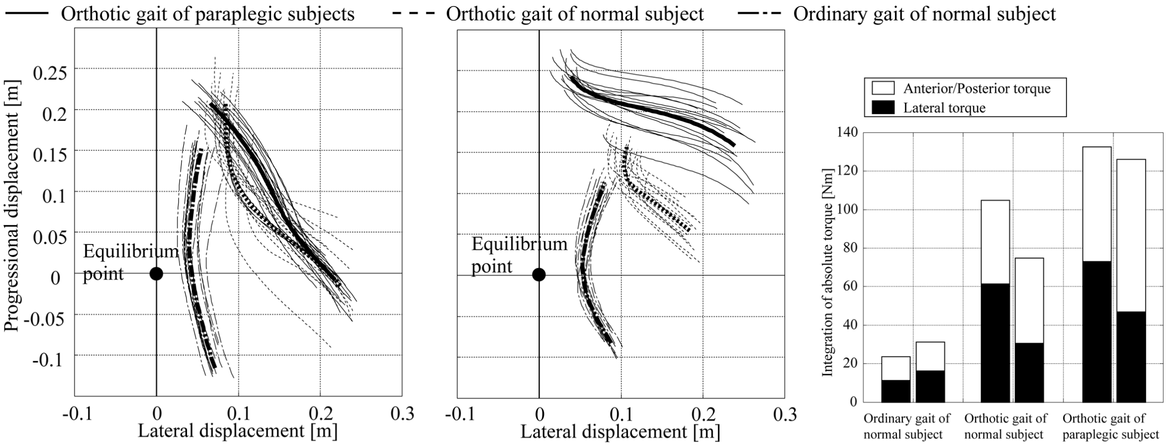

(a) Lumbar joint trajectories in large stride (b) Lumbar joint trajectories in small stride (c) Integrated absolute torque

Fig. 6. Results of analyses for lumbar joint trajectories using the inverted pendulum model. (a) and (b) show the trajectories in the horizontal plane while left single support phase. (c) shows integrated absolute torque for mean trajectories.

and farther to the equilibrium point in the lateral direction than the ordinary gait of the normal subject. The integrated torque values are shown in Fig. 6(c). The white and black bars indicate the values of the progressional and lateral torque, respectively. The integrated value is lowest in the ordinary gait of the normal subject and highest in the orthotic gaits of the paraplegic subjects. For larger lateral displacement in the orthotic gait, not only the lateral torque but also the progressional torque increased. The direction of progressional torque decelerates rather than accelerates the point of mass moving forward.

3.2.2 Analysis of the trajectory direction angle

Figure 7 shows the lumbar joint trajectories for various trajectory direction angles δ. δ was set from –60 to 60° at intervals of 20°. δ_{MT} is the direction angle for the mean trajectories, shown by solid lines, and the dashed lines are the minimum jerk trajectories for various values of δ. δ_{MT} has negative values in the orthotic gait of the normal subject, in which the lateral peak occurs during the single support phase, and positive values in the orthotic gait of the paraplegic subjects. The minimum jerk trajectories with δ_{MT} coincide with the mean trajectories. The trajectories for paraplegic subject 1 and the normal subject were curved with the parameter value of δ. The variety of paraplegic subject 2 is smaller than those of the other subjects because the displacement of the progressional direction is small for the lateral displacement.

Figure 8 shows the integrated torque of the trajectories shown in Fig. 7. The integrated torque of the minimum jerk trajectories with δ_{MT} (JT) coincided with that of the mean trajectories (MT) for all of the subjects. The integrated torque is lowest at $\delta = 0°$ for paraplegic subject 1 and in the large stride gait of the normal subject. It is lowest for $\delta = –20°$ in the small stride gait of the normal subject, and for $\delta = 40°$ in the small stride gait of paraplegic subject 2.

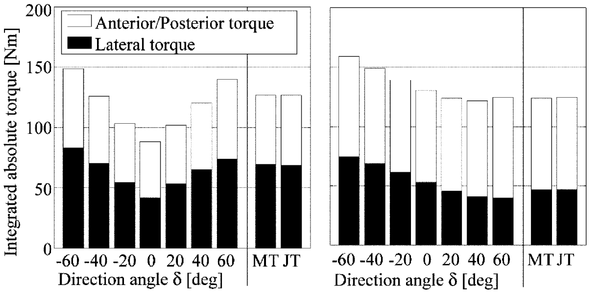

(a) Paraplegic subject 1 (b) Paraplegic subject 2

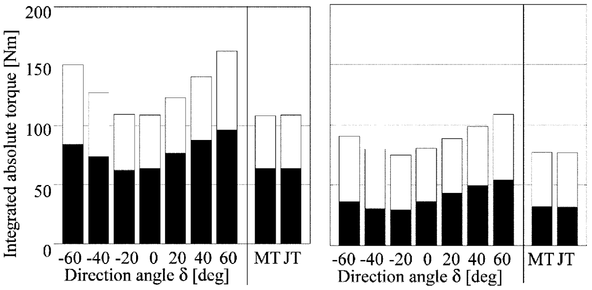

(c) Normal subject 3 (large stride) (d) Normal subject 3 (small stride)

Fig. 8. Integrated absolute torque in lateral and anterior/posterior direction for the calculated trajectories from δ, mean trajectories and minimum jerk trajectories. The results from (a) to (d) correspond to the trajectories in Fig. 7.

In the orthotic gait of the normal subject, the value of δ at which the integral torque is minimum corresponds to δ_{MT}. In the orthotic gait of paraplegic subject 1, the inte-

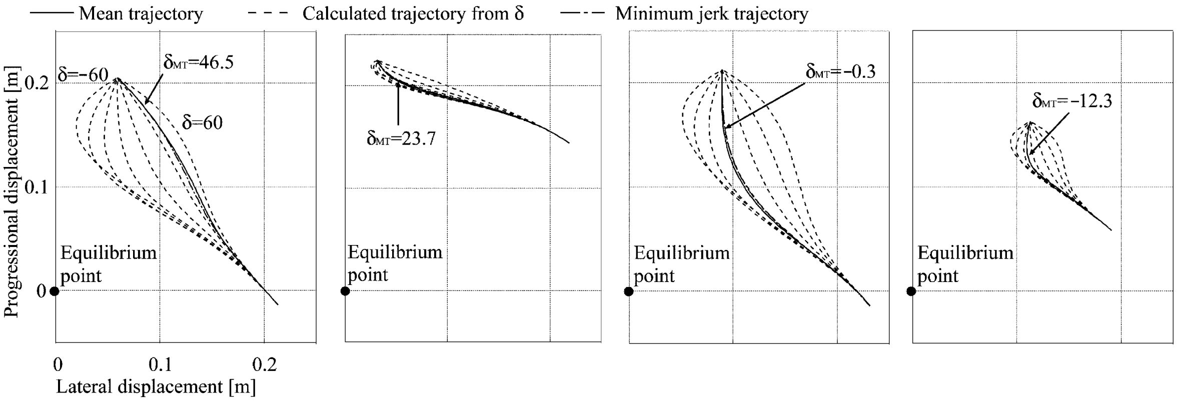

(a) Paraplegic subject 1 (b) Paraplegic subject 2 (c) Normal subject 3 (large) (d) Normal subject 3 (small)

Fig. 7. Calculated lumbar joint trajectories from δ. (a) Subject 1 (paraplegia, large stride); (b) subject 2 (paraplegia, small stride); (c) subject 3 (normal, large stride); (d) subject 3 (normal, small stride).

gral torque of δ_{MT} has higher values than that of the curved trajectory in the direction of the equilibrium point.

3.3 Discussion

Applying the measured lumbar joint trajectories to an inverted pendulum model, the trajectories of the ordinary gait of the normal subject were located near the unstable equilibrium point. The trajectories of the orthotic gait were located anterior to the equilibrium point. Quantifying the contribution of the external force by the integrated torque, the value is lowest in the ordinary gait of the normal subject and highest in the orthotic gaits of the paraplegics. Comparing the shape of the trajectories in the orthotic gaits of the paraplegics with that in the orthotic gait of the normal subject, the value of the external force contribution for curved trajectories, such as that of the normal subject, is lower than in the rectilinear such as those of the paraplegic subjects.

In this analysis, the contribution of external force, such as effort of the upper extremities, is quantified by the integrated torque acting on the degrees of freedom of the inverted pendulum. This agrees with the finding of previous studies that the ordinary gait of normal people is more efficient than the orthotic gait of paraplegics [11]. The shape of the trajectory was parametrized by means of the trajectory direction angle at heel contact δ, and we analyzed the relationship between the integral torque value and the trajectory direction angle. The coincidence between the mean trajectories and the minimum jerk trajectories with δ_{MT} indicates that the trajectory representation based on minimum jerk model is reasonable. The optimal value of δ is determined by the following trade-off relationship: the moment of gravity increases when the distance between trajectory and the equilibrium point is large, and the moment of inertia increases when the length of trajectories is large. The rectilinear trajectories show larger moments of gravity and smaller moments of inertia than the curved trajectories. These results suggest that the trajectories of the orthotic gait of the normal subject were curved so that the effort of the upper extremities was minimized for this trade-off. The features of the lumbar joint trajectories in the ordinary gait of the normal subject, located near the equilibrium point, depend on the gravity field of the inverted pendulum and sufficient progressional velocity at toe-off [9, 11]. The restriction of the ankle joint prevents acceleration of the body center of mass in the preswing phase. The restrictions of the ankle joint in dorsiflexion and of the knee joint in the complete flexion position prevent backward loss of balance, since the body's center of mass is located anterior to the support foot position. However, the stride length was limited since the lumbar joint trajectories were located anterior to the equilibrium point. Moreover, a large lateral displacement toward the equilibrium point is required to keep sufficient foot-floor clearance. As the internal/external rotation of the hip joints is restricted at a slightly external position and the lumbar joint is far from the equilibrium point, a margin with respect to the base of support was obtained for the lateral displacement. However, the large lateral displacement against gravity increases the arm loading. As shown by Nene and Major, the lateral displacement against the gravity moment requires a large external force [7]. In addition to the lateral torque, the backward torque increases, resisting the progressional moment by the gravity. Therefore, it has been suggested that leg restriction prevented backward loss of balance, while increasing the arm loading.

Our analysis for subject 1 revealed that the integrated torque of the curved trajectory in the direction of the equilibrium point was lower than that of the rectilinear trajectory. The external force of the curved trajectory increased for paraplegic subject 2. This difference caused a small movement duration which affected the inertial force rather than the gravity force. As the trajectories of paraplegic subject 2 were farther from the equilibrium point than other subjects, his minimum value for parameter δ was the largest in the other conditions. These results suggest that the increase in the distance between the trunk movement and the supporting foot results in significant loading in the orthotic gait of paraplegics.

In ambulation with an MSH-KAFO type orthosis, the lateral displacement of the trunk is larger than in the normal gait. This result coincides with the ambulation with HKAFO reported by Jefferson and Whittle [8]. The lateral displacement in MSH-KAFO is caused not only by the fixation of the knee joint but also by the trunk position located anterior to the supporting foot position at toe-off, because the lateral movement is required to peak in the vertical direction during the single support phase.

In previous studies, the kinematics and dynamics of the orthotic gait have been analyzed separately [7, 8]. In this study, we analyze the kinematic differences due to leg restriction and motor paralysis on the basis of a dynamical model of an inverted pendulum model. Based on the results of our analysis, improvements of the orthotic gait are discussed below.

To decrease the loading of the crutches in the orthotic gait of paraplegics, improvements of the orthosis and design of power-assist devices are necessary in order to assure that the trunk movement is located near the supporting foot. In the ordinary gait of normal subjects, the lumbar joint trajectories during the single support phase are located near the supporting foot position, which corresponds to the equilibrium point. In addition, the lumbar joint position at toe-off is located posterior to the equilibrium point and the lateral peak position is close to the equilibrium point. The velocity at toe-off is sufficiently large for forward progression, since the plantar flexors of the ankle joint and the extensors of the hip joint in the preswing phase are activated. In the orthotic gait of paraplegics, since motor paralysis of the muscles related to the ankle and hip joints limits the velocity of the gait, improvement of efficiency approximating that of normal persons would not be achievable by any instruction or training.

A method of preventing backward loss of balance is required in order to perform an efficient gait like that of normal people, in which the trunk at toe-off is located posterior to the supporting foot. If the same method as used by normal people is implemented, large actuators would be required to provide sufficient progressional velocity at toe-off. To compensate the backward loss of balance, instead of the mechanism of normal people, improvements of the shape of the sole of the foot, crutches, and a rollator might be effective. In addition, sufficient foot-floor clearance produced by actuators [14] and narrowing of the width of stance would decrease the lateral displacement, which is a factor in the significant arm loading.

The orthotic gait of paraplegic subject 1 has a rectilinear shape and is distant from the supporting foot position. To perform a curved trajectory, the velocity of lateral movement at toe-off should increase as in the orthotic gait of the normal subject. An improvement of the pelvis corset increasing the stiffness of lateral flexion might be effective in decreasing the influence of trunk motor paralysis and in controlling the lateral displacement. Instruction in the performance of curved trajectories might accelerate motor learning and help to decrease arm loading. In the orthotic gait of paraplegic subject 2, the external force is large due to the position of the trunk, located significantly anterior to the supporting foot. As the ankle joint angle is set in a slightly more dorsiflexed position, a sufficient base of support with respect to the posterior direction would be required to increase the stride length and decrease the arm loading.

4. Conclusions

In this study, we address the relationship between significant arm-clutch loading, leg restriction, and motor paralysis, compared with the lumbar joint trajectories in the orthotic gaits of paraplegic subjects and the ordinary and orthotic gaits of a normal subject using an inverted pendulum model. The influences on the differences in trajectory were analyzed using an inverted pendulum model, and the contribution of external forces was discussed in terms of the relationship between the trajectories and the equilibrium point. The results of this analysis are summarized as follows.

- Influence of leg restriction: The restriction of the ankle joint at a slightly dorsiflexed position and of the knee joint at complete extension cause the trunk to be located anterior to the supporting foot, and the large reaction force of the crutches is required to resist the lateral and progressional moment of gravity.
- Influences of motor paralysis: Due to motor paralysis of the trunk joint, the shape of the lumbar joint trajectories is rectilinear in the orthotic gait of paraplegics. The large reaction force of the crutches is required to perform a rectilinear trajectory because the distance between the trajectory and the equilibrium point is large.

These results suggest that the increased distance between the trunk movement and the equilibrium point of the inverted pendulum results in significant loading due to leg restriction and motor paralysis in the orthotic gait of paraplegics.

Acknowledgments

We thank Professor Eiichi Saitoh and Dr. Keiko Onogi, M.D., of Fujita Health University and Assistant Professor Naohiro Fukumura of Toyohashi University of Technology for their valuable comments and assistance in our investigation. This research was supported under the “Basic Technology Development for Practical Application of Human Support Robots” program of the New Energy and Industrial Technology Development Organization (NEDO) and the 21st Century COE Program “Intelligent Human Sensing” of the Ministry of Education, Culture, Sports, Science and Technology of Japan.

REFERENCES

1. Heruti R, Ohry A. Some problems of the lower extremities in patients with spinal cord injuries. International Journal of Lower Extremity Wounds 2003;2:99–106.
2. Yano H. Gait orthoses for paraplegics. Journal of Clinical Rehabilitation 2003;12:946–950. (in Japanese)
3. Tsuzuki A, Teranishi T, Saitoh E. Standing and gait orthosis for spinal cord injured. In: Prosthesis and orthosis in rehabilitation medicine. Kanehara & Co.; 2003. p 167–172. (in Japanese)
4. Rose GK. The principle and practice of hip guidance articulations. Prosthetics and Orthotics International, No. 3, p 37–43, 1979.

5. Douglas R, Larson PF, D'Ambrosia R, McCall R. The LSU reciprocation-gait orthosis. Orthopedics, No. 6, p 834–839, 1983.
6. Suzuki T, Sonoda S, Saitoh E, Onogi K, Fujino H, Teranishi T, Oyobe T, Katoh M, Ohtsuka K. Prediction of gait outcome with the knee-ankle-foot orthosis with medial hip joint in patients with spinal cord injuries: A study using recursive partitioning analysis. Spinal Cord 2007;45:57–63.
7. Nene AV, Major RE. Dynamics of reciprocal gait of adult paraplegics using the ParaWalker (hip guidance orthosis). Prosthetics and Orthotics International, No. 11, p 124–127, 1987.
8. Jefferson RJ, Whittle MW. Performance of three walking orthoses for the paralysed: A case study using gait analysis. Prosthetics and Orthotics International, No. 14, p 103–110, 1990.
9. Zajac FE, Neptune RR, Kautz SA. Biomechanics and muscle coordination of human walking. Part II. Lessons from dynamical simulation and clinical implications. Gait and Posture 2003;17:1–17.
10. Perry J. Gait analysis. Slack; 1992. p 131–140.
11. Kooij H, Jacobs R, Koopman B, Herm F. An alternative approach to synthesizing bipedal walking. Biol Cybern 2003;17:46–59.
12. Paul RP. Robot manipulators: mathematics, programming and control. MIT Press; 1985.
13. Flash T, Hogan N. The coordination of arm movement: An experimentally confirmed mathematical model. J Neurosci 1985;5:1688–1703.
14. Goldfarb M, Durfee WK. Design of a controlled-brake orthosis for FES-aided gait. IEEE Trans Rehab Eng 1996;4:13–24.

APPENDIX

1. Calculation of Joint Position

A homogeneous transform representation is used to calculate the joint position defined in Fig. 2 from the measured marker position data. The homogeneous transform representation is suitable for describing the state of the linkage structure in a 3D workspace. The position vector is represented as the following 4D vector form:

$$\boldsymbol{r} = [ax, ay, az, a]^T \qquad \text{(A.1)}$$

where a is a scale factor. The vector $\boldsymbol{r}$ does not depend on the value of a. Its value is set as 1 in the following. The homogeneous transform matrix represents the position and attitude of a link in the workspace, and performs the transformation from the position vector ${}^L\boldsymbol{r}$ in the link coordinate system $\Sigma_L(0_L - X_L Y_L Z_L)$ to the position vector ${}^U\boldsymbol{r}$ in the workspace coordinate system $\Sigma_U(0_U - X_U Y_U Z_U)$. Figure A.1(a) illustrates the workspace coordinate system and the link coordinate system, where ${}^U\boldsymbol{r}_L$ represents the origin and ${}^U\boldsymbol{n}_L$, ${}^U\boldsymbol{o}_L$, and ${}^U\boldsymbol{a}_L$ are unit vectors representing the direction of the longitudinal (X), lateral (Y), and anterior/posterior (Z) axes of the linkage in the workspace coordinate system. Based on this definition, the homogeneous transform matrix of the link coordinates in the workspace coordinate system is given by

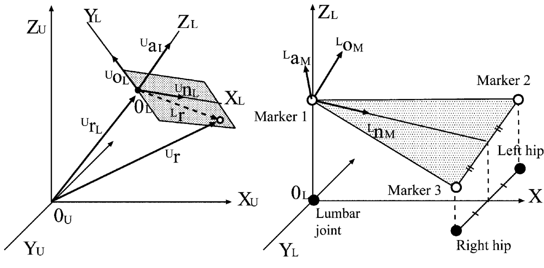

(a) Link coordinates (b) Marker coordinates in pelvis

Fig. A.1. Link and marker coordinates. (a) The link coordinates for the work space coordinates. (b) The marker coordinates for the pelvis link coordinates.

$$ {}^U\boldsymbol{H}_L = \begin{bmatrix} {}^U(n_x)_L & {}^U(o_x)_L & {}^U(a_x)_L & {}^U(r_x)_L \\ {}^U(n_y)_L & {}^U(o_y)_L & {}^U(a_y)_L & {}^U(r_y)_L \\ {}^U(n_z)_L & {}^U(o_z)_L & {}^U(a_z)_L & {}^U(r_z)_L \\ 0 & 0 & 0 & 1 \end{bmatrix} \qquad \text{(A.2)}$$

The position in workspace coordinates ${}^U\boldsymbol{r}$ is related to the position in link coordinates by the transformation matrix ${}^U\boldsymbol{H}_L$:

$$ {}^U\boldsymbol{r} = {}^U\boldsymbol{H}_L({}^L\boldsymbol{r}) \qquad \text{(A.3)}$$

The transformation matrices of the body segments cannot be calculated directly from the measured position data because the markers were attached to the body surface. Therefore, the parameters of the marker positions in the link coordinate of the depth (Z axis) are defined. From these parameter values, the homogeneous transformation matrices from the link coordinates to the marker coordinates were defined. Figure A.1(b) illustrates the relationship between the link coordinates and marker coordinates. The longitudinal axis (X) is defined as the direction of the segment consisting of marker 1 and the midpoint of the segment between markers 2 and 3. The anterior–posterior axis (Z) is defined as the direction of the normal vector of the plane spanned by markers 1, 2, and 3. The transformation matrix ${}^L\boldsymbol{H}_M$ for the pelvis is obtained similarly to Eq. (A.2). The transformation matrix from marker coordinates into the workspace coordinates ${}^U\boldsymbol{H}_M$ is calculated from the measured position data. From the matrices ${}^L\boldsymbol{H}_M$ and ${}^U\boldsymbol{H}_M$, the transformation matrix ${}^U\boldsymbol{H}_L$ is obtained as follows:

$$ {}^{U}\boldsymbol{H}_L = {}^{U}\boldsymbol{H}_M ({}^{L}\boldsymbol{H}_M)^{-1} \tag{A.4} $$

Once ${}^{U}\boldsymbol{H}_L$ of the pelvis is obtained, the positions of the lumbar joint and hip joints corresponding to the origin-adjacent links (the trunk and the left and right thighs) can be calculated from Eq. (A.3). The homogeneous transform matrices of the adjacent links are obtained from the origin positions of the links, the measured marker positions, and the marker position parameters in link coordinates, and likewise for the pelvis. Repeating this procedure, the homogeneous transform matrices of all body segments are obtained.

Considering the relationship between the marker positions and body segments, and the foot-floor clearance restricted joint movements of legs, the parameter values of the marker positions of the link coordinates were adjusted by trial and error.

2. The 3D Inverted Pendulum Model

With respect to the inverted pendulum model defined as Fig. 5(b), the transformation from the joint angles ($\boldsymbol{q} = [\theta, \psi]^T$) to the position of the point of mass ($\boldsymbol{r} = [x, y, z]^T$) is expressed by the following equation (forward kinematics):

$$ x = L\mathrm{c}_\theta \mathrm{c}_\psi \tag{A.5} $$

$$ y = L\mathrm{s}_\psi \tag{A.6} $$

$$ z = -L\mathrm{s}_\theta \mathrm{c}_\psi \tag{A.7} $$

where $s_{\theta,\psi}$ and $c_{\theta,\psi}$ are the sine and cosine of θ and ψ. The transformation from the position of the point of mass to the joint angle is as follows (inverse kinematics):

$$ \theta = \mathrm{atan2}(-z, x) \tag{A.8} $$

$$ \psi = \mathrm{atan2}(y, x\mathrm{c}_\theta - z\mathrm{s}_\theta) \tag{A.9} $$

where the arctangent function "atan(a, b)" gives the angle whose sine equals a, and whose cosine equals b. The velocity of the point of mass $\dot{\boldsymbol{r}}$ is calculated from the angular velocity $\dot{\boldsymbol{q}}$ by the equations

$$ \dot{\boldsymbol{r}} = \boldsymbol{J}\dot{\boldsymbol{q}} \tag{A.10} $$

$$ \boldsymbol{J} = \begin{bmatrix} -L\mathrm{s}_\theta \mathrm{c}_\psi & -L\mathrm{c}_\theta \mathrm{s}_\psi \\ 0 & -L\mathrm{c}_\psi \\ -L\mathrm{c}_\theta \mathrm{c}_\psi & -L\mathrm{s}_\theta \mathrm{s}_\psi \end{bmatrix} \tag{A.11} $$

Since the equations of motion were obtained by the Lagrange method, the inertial matrix, the Coriolis-centrifugal term, and the gravity term in Eq. (3) are expressed as follows:

$$ \boldsymbol{M} = \begin{bmatrix} ML^2\mathrm{c}_\psi^2 & 0 \\ 0 & ML^2 \end{bmatrix} \tag{A.12} $$

$$ \boldsymbol{V} = \begin{bmatrix} -2ML^2\dot{\theta}\dot{\psi}\mathrm{s}_\psi \mathrm{c}_\psi \\ ML^2\dot{\theta}^2\mathrm{s}_\psi \mathrm{c}_\psi \end{bmatrix} \tag{A.13} $$

$$ \boldsymbol{G} = \begin{bmatrix} -MgL\mathrm{c}_\theta \mathrm{c}_\psi \\ MgL\mathrm{s}_\theta \mathrm{s}_\psi \end{bmatrix} \tag{A.14} $$

where M denotes the mass of the body and g denotes the acceleration of gravity.

AUTHORS (from left to right)

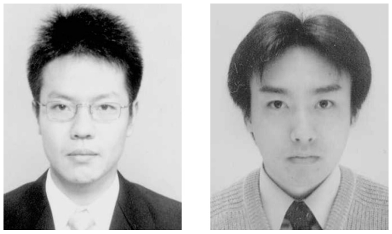

Takahiro Kagawa (member) received his Ph.D. degree in engineering from Toyohashi University of Technology in 2006. He became a research associate in the Department of Biosciences and Informatics at Keio University and is now affiliated with the Keio Tsukigase Rehabilitation Center.

Hiroshi Fukuda (nonmember) received his Ph.D. degree in engineering from Toyohashi University of Technology in 2001 and became a research associate in the Department of Information and Computer Sciences.

AUTHORS (continued)

Yoji Uno (nonmember) received his Ph.D. degree in engineering from Osaka University in 1988 and became a research associate in the Department of Mathematical Engineering and Information Physics at the University of Tokyo, and a lecturer in 1991. In 1992, he joined the Advanced Telecommunications Research Institute (ATR) as a senior researcher. He later became a professor at Toyohashi University of Technology, and is now a professor in the Department of Mechanical Science and Engineering at Nagoya University. His research interests are in biological motor systems.

Copyright of Electrical Engineering in Japan is the property of Wiley Periodicals, Inc. 2004 and its content may not be copied or emailed to multiple sites or posted to a listserv without the copyright holder's express written permission. However, users may print, download, or email articles for individual use.

Copyright of Electrical Engineering in Japan is the property of Wiley Periodicals, Inc. 2004 and its content may not be copied or emailed to multiple sites or posted to a listserv without the copyright holder's express written permission. However, users may print, download, or email articles for individual use.